#3543

VA-89-2-3

A Model to Compare Freezing Control Strategies for Residential Air-to-Air Heat Recovery Ventilators

E.G. Phillips, P.E. **R.E. Chant, P.E.** **B.C. Bradley, P.E.** **D.R. Fisher, P.E.**

ABSTRACT

A computer program was developed to simulate the performance of residential air-to-air heat recovery ventilators of various effectivenesses operating under frosting conditions. Algorithms were developed to predict the energy performance of the heat recovery ventilators for several frost control and defrost strategies for any prescribed climatic conditions. This paper describes the weather model, the heat exchanger performance/frosting model, and the defrost and frost control algorithms developed for this ASHRAE-funded project.

INTRODUCTION

Air-to-air heat exchangers with built-in fans and controls (now called heat recovery ventilators or HRV) form an energy-efficient ventilation system in many houses. In cold weather, ice or frost form on exhaust-side surfaces of the heat exchanger, reducing heat recovery in two ways:

1. Frost "fouls" heat exchange surfaces, reducing thermal conductance and thus heat transfer rates, and
2. Frost blocks exhaust airflow passages, reducing the energy available for recovery.

As a result, HRV manufacturers have incorporated strategies to prevent or limit the build-up of frost in heat exchangers. However, little has been done to analytically compare the effect of these strategies on the seasonal performance of HRV under different climatic conditions.

ASHRAE T.C.-5.5-sponsored research project TRP 543, "An Investigation of Freezing Control Strategies for Residential Air to Air Heat Exchangers," had the following objectives:

1. To analytically characterize freeze-control strategies used for residential air-to-air heat exchangers (HRV).
2. To compare the need for, and effect of, various freeze-control strategies on the seasonal thermal performance of residential heat recovery units operating in different climates.
3. To optimize specific freeze-control strategies and evaluate the associated energy savings.

For this project, a literature review was completed to assemble background information on freeze control strategies and a computer program was developed to provide a standardized energy performance comparison of HRV freeze control strategies under different climatic conditions. This paper describes the computer program. The results of this study are presented elsewhere (Phillips et al. 1989).

In this paper, freeze control strategies are classified as frost control strategies (i.e., methods or mechanisms that prevent frost from forming in the heat exchanger such as preheating supply air temperatures above the frost threshold temperature) and defrost strategies (i.e., methods or mechanisms that routinely remove frost from the heat exchange core to restore heat recovery and ventilating performance such as periodically melting frost and ice by turning off the supply air fan while continuing to run the exhaust fan).

LITERATURE REVIEW

Early literature (pre-1975) provided information on frosting based on heat exchangers such as refrigerating evaporators and cryogenic applications. It included the following:

1. Theoretical models related the thermal conductivity of frost to its density (Jones and Parker 1975; Yonko and Sepsy 1967).
2. Theoretical expressions for density and thermal conductivity of frost predicted the values within

E.G. Phillips and **B.C. Bradley** are Engineering Consultants with UNIES Ltd., Winnipeg, MB, Canada; **R.E. Chant** is Professor of Mechanical Engineering, University of Manitoba, Winnipeg; **D.R. Fisher** is a Consulting Engineer in Danville, CA.

25% of values measured under a variety of environmental conditions including humidity, velocity, and surface temperature (Bigura and Wenzel 1970).

3. The rate of frost formation (that is, the full development of the crystalline structure on a surface), although velocity-dependent, is relatively rapid (Kamei et al. 1952).

4. The properties of frost formation are dependent on the history of the formation and there is a need for studies of the frost forming under varying environmental conditions (Schneider 1978; Yonko and Sepsy 1967).

The detailed mechanisms of frost formation have been studied using photographic techniques and established structural model formations (Hayashi et al. 1977). However, there is sufficient information in the literature to predict the growth rates and the thermal conductivity of frosting to enable an analytical study to be performed.

The only reported investigations on the performance of an air-to-air heat exchanger during freezing and during freezing with periodic defrost cycles were in the work of a national laboratory (Fisk et al. 1983; Fisk et al. 1985a). The engineering science department of a U.S. university (Alexander 1986) reported on tests covering seasonal performance in which a seasonal performance of 90% was obtained. However, despite the climatic conditions, there is no evidence of frosting occurring, since the vents were closed on cold nights. The Ministry of Energy, Province of Ontario (1987), has reported on some seasonal in situ monitoring of units equipped with defrost mechanisms. Several maintenance problems were encountered; thus the results are far from conclusive. These latter reports use a multiplicity of expressions for effectiveness, sensible effectiveness, heat recovery efficiency, etc., and thus point out a need for standardization of nomenclature. The reported investigations to date also point out a need for controlled seasonal performance tests.

To estimate the seasonal performance of HRV in the analytical study performed herein, annual bin climatic data were built up for each month using the method developed by Erbs et al. (1983). Again a need to determine the actual energy recovered as a percentage of the total actual energy available for certain climatic regions on an annual basis is apparent.

PROGRAM DESCRIPTION

The analytical study of frost control and defrost strategies requires:

1. Information that relates airstream conditions and heat exchanger parameters to energy performance over time,
2. Temperature data for the locations to be studied, and
3. Algorithms for the defrost and frost control strategies to be studied.

The computer program developed for this study contained:

1. A heat exchanger frosting model,
2. A temperature bin data generator, and
3. Defrost and frost control algorithms.

The HRV frosting model simulated one hour of heat exchanger operation at various outdoor temperatures, without operation of a defrost or frost control mechanism. HRV performance data were calculated and recorded at one-minute time-steps.

The temperature bin data generator was used to estimate the number of hours in each temperature bin for the location selected in each climate zone. Simulations were done at temperatures corresponding to the middle of each bin. Temperature bins were 2°C (3.6°F) wide.

The outputs from the HRV frosting model and temperature bin data were input into a "post processor," which contained the defrost and frost control algorithms. The post processor used these inputs to generate standardized seasonal performance data for each combination of HRV/climate/freeze control for a generic counterflow heat exchanger configuration.

HEAT EXCHANGER MODEL

For this study, a finite difference model that could predict the amounts and location of frost and ice in the heat exchanger was developed. In the model, the heat exchange core was subdivided into a series of heat transfer cells (typically 30 cells). Heat exchanger operation was simulated over a range of outdoor temperatures. At each temperature, energy performance calculations were done in time-steps (typically, one minute). Within each time-step, heat transfer computations were made cell by cell, beginning at the warm end of the heat exchanger and proceeding through to the cold end.

A counterflow heat exchanger configuration was modeled, since it was the most easily simulated heat exchanger configuration. The heat exchange surface area used was based on "typical" surface areas of production HRV of similar effectiveness. Heat transfer coefficients were selected so the predicted temperature effectiveness under non-freezing conditions was equal to the nominal effectiveness of the HRV to be evaluated.

Four distinct air/moisture regimes or regions can occur as exhaust air is cooled from its inlet conditions to its outlet conditions (see Figure 1, from Besant and Bugg [1982]). First is a dry region, in which the exhaust air temperature is above its dew point. Second is a region in which there is condensation from the exhaust air. It was assumed that condensation was cooled to the temperature of the heat exchange core in the cell in which the condensation occurred. In the third region, heat exchange surfaces are below freezing and exhaust air is above freezing. Condensation freezes to ice at the core temperature for that cell. In the fourth region, exhaust air temperature is below 32°F (0°C) and condensation from the exhaust air forms frost at the core temperature of the cell. Different heat exchange equations were required to simulate each of the four air/moisture conditions.

At low outdoor temperatures, supply airflow passages remain dry because the supply air temperatures increase as the air passes through the heat exchanger.

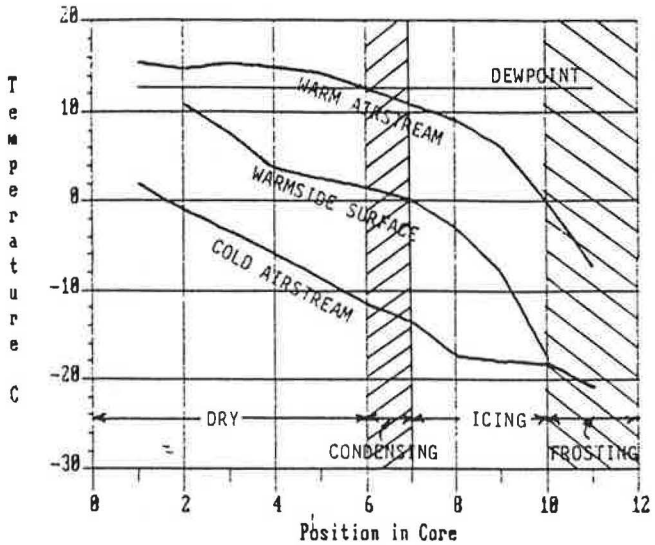

Figure 1 *Illustration showing the locations of the dry, condensing, icing, and frosting regions in an HRV*

The location of each region varies with inlet airstream conditions, airflow rates, and heat exchanger parameters (including heat exchange area and heat transfer coefficients, which are, in turn, affected by the amount and location of ice or frost in the heat exchange core).

The amount of energy transferred in a cell in a particular time-step was estimated as:

$$Etrans = UA\Delta Tt \quad (1)$$

where

- U = heat transfer coefficient for the heat exchanger core in that cell and that time-step
- A = area of heat exchanger surface in the cell
- T = the mean temperature difference between the supply air temperature and the exhaust air temperature in that cell
- t = time-step duration

The enthalpy change in a cell for a non-condensing airstream was estimated as follows:

$$mdH = Etrans \quad (2)$$

$$so,\ dH = Etrans/m \quad (3)$$

$$and,\ dW = 0 \quad (4)$$

where

- m = mass flow rate of the airstream
- dH = enthalpy change of the airstream in that cell
- $Etrans$ = energy transferred to or from that cell
- dW = change in moisture content for the airstream

For airstreams with condensation, *Etrans* was made up of an enthalpy change in the airstream plus the sensible and latent energy required to cool and freeze (where applicable) the condensation to the heat exchanger core temperature. A description of the procedure for estimating the energy from each source and the condensation in each cell/time-step is presented below, and supported with the psychrometric chart illustration in Figure 2.

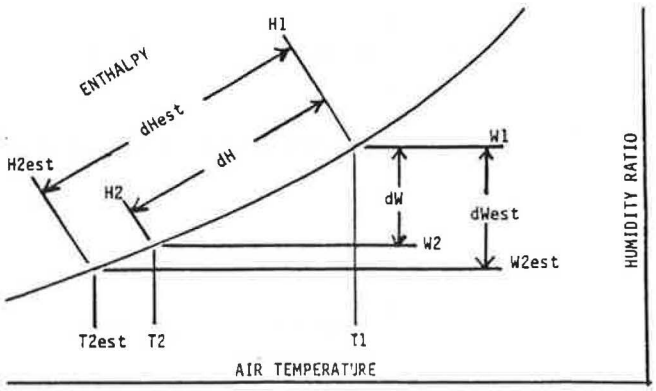

Figure 2 *Psychrometric chart illustration*

1. $dHest = H1 - H2est = UA\Delta Tt \quad (5)$

$$H2est = H1 - UA\Delta Tt/m \quad (6)$$

where

- $dHest$ = a first estimate of the change in the enthalpy of the airstream in that cell/time-step
- $H1$ = the enthalpy of the airstream at the warm side of the cell in that timestep. The value for $H1$ for the cell/time-step is known.
- $H2est$ = an initial estimate of the enthalpy of the airstream at the cold side of the heat exchanger

2. The estimated change in humidity ratio (*dWest*) is related to the estimated change in enthalpy of the airstream (*dHest*). *dWest* was determined using standard ASHRAE psychrometric equations.

3. The energy needed to the cool the condensation from a unit of air at the mean airstream temperature in the cell to the heat exchanger core temperature was calculated by:

$$deW = dWest \cdot dhW \quad (7)$$

where

- deW = the energy needed to cool condensation to the heat exchanger core temperature
- $dWest$ = the change in humidity ratio related to a change in airstream enthalpy from $dH1$ to $dH2est$
- dhW = the change in enthalpy for water cooled from the mean estimated airstream temperature to the cell core temperature

4. Estimate the fraction of energy transferred, which is due to a change in enthalpy of the air.

$$F = dHest/(dHest + deW) \quad (8)$$

where

- F = the fraction of energy recovered from the enthalpy change of air

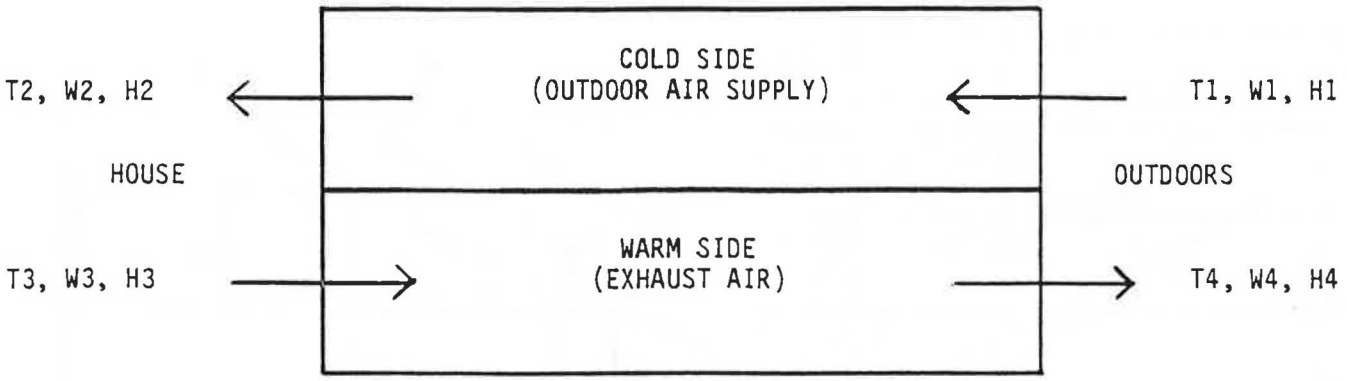

Figure 3 *Airstream numbering convention*

5. The actual amount of energy recovered from the airstream in that cell/timestep was then estimated as:

$$Eair = F(UA\Delta Tt) \quad (9)$$

where

Eair = the energy recovered from the airstream

Airstream conditions at the cold side of the cell and the amount of condensation are easily found by using the psychrometric equations.

For the range of conditions that could occur in the simulations, the value of *F* was virtually constant within a cell/time-step. *F* is directly related to the slope of the saturation curve on the psychrometric chart or, more precisely, the relationship between the humidity ratio lines and enthalpy lines along that curve (i.e., *dW/dH*). In the most extreme condition simulated (i.e., 80% heat exchanger effectiveness, −65°F [−54°C] outdoor temperature, exhaust air at the warm side of the cell at its saturation temperature of 45°F [7.2°C] air, and condensation being cooled below freezing), the first estimate for temperature drop for air passing through a cell is 3.6°F (2.0°C). The final value was 3.3°F (1.8°C). Whereas there is an 8.1% difference in enthalpy between the first estimate and the final value, the change in *dW/dH* related to this enthalpy difference is 0.245% for this most extreme condition.

Starting Conditions

The heat exchange core was divided into heat transfer cells and the outdoor temperature was selected. In the first time-step the heat exchanger was assumed to have clean heat exchange surfaces. The beginning supply air temperature to the house, *T2* (the conventional airstream numbering system, as illustrated in Figure 3, is used in this paper), was estimated as:

$$T2est = e\,(T3 - T1) + T1 \quad (10)$$

where

T1 = bin temperature (i.e., cold-side inlet air temperature)
T2est = temperature estimate for HRV supply to the house (i.e., cold-side outlet air temperature)
T3 = inlet temperature of exhaust air (i.e., warm-side inlet temperature)
e = nominal heat exchanger effectiveness

T2est, *T1*, and the mass flow rate were used to estimate the energy recovered. An estimate of the exhaust airstream exit temperature, *T4est*, was made using *T3*, the estimate of energy recovered and the exhaust airstream mass flow rate. Initial temperature profiles were generated for the cold-side air temperatures in each cell.

For the exhaust airstream, the air temperature at the cold side of cell *n* was estimated as:

$$ETcn = T3 - n(T3 - T4)/N \quad (11)$$

For the supply airstream, the air temperature at the cold side of cell *n* was estimated as:

$$STcn = T2 - n(T2 - T1)/N \quad (12)$$

Cell-by-Cell Calculations

Calculations began at the warm end of the heat exchanger. Mean temperatures for each airstream were estimated by averaging the temperatures for the warm side and the cold side of the cell. For the first cell, *T2est* and *STc*1 were used for the supply airstream and *T3* and *ETc*1 for the exhaust airstream. Heat transfer for the cell was estimated using the mean airstream temperatures in the cell. An energy balance and new cold-side conditions (temperature, enthalpy, humidity ratios) were calculated for the airstreams at the cold side of the cell. These cold-side temperatures became the warm-side temperatures for the next cell, while the temperatures generated for the cold-side profiles were used for the cold side.

Any condensation was assumed to be cooled down to the heat exchange core temperature. The heat exchanger core temperature was assumed to be the average of the mean airstream temperatures in the cell. The energy to cool (and freeze, if appropriate) this moisture was factored into the energy balance and the respective airstream conditions, as previously discussed.

This procedure was repeated for each cell using the calculated cold-side conditions from the previous cell as the warm-side conditions for the current cell. The energy recovered, condensate mass and frost or ice mass, temperature, and thickness in each cell and the time-step were recorded.

Checking for Convergence

Once the calculations were performed for all cells, the temperature predicted for the supply airstream at the cold end (i.e., the inlet) of the heat exchanger was compared to

the bin temperature, *T1*. If the difference in temperatures was less than the specified tolerance limit (i.e., 0.09°F [0.05°C]) the simulation was considered acceptable. Otherwise an adjustment was made to *T2est* and the time-step was rerun using the cold-side cell temperatures generated in the previous iteration. This process was repeated until the simulation temperature for the exhaust air inlet fell within the tolerance limit.

Next Time-Step

The frost and ice thicknesses recorded for each cell in the last iteration of one time-step were used to reduce the heat conductance for that cell in the next time-step. A second adjustment was made to account for airflow reductions due to frost blockage. The cold-side air temperature profiles from the last iteration of the previous time-step were used for the first iteration of the current time-step. The cell-by-cell process was then repeated for this new set of conditions.

Termination of a Simulation

The simulation at an outdoor temperature was terminated when one of the following conditions was met:

- steady-state was reached (i.e., when the rate of increase in frost and ice accumulation was negligible. This would occur after the first time-step for temperatures at which frosting was not encountered).
- the greatest frost thickness in any cell exceeded a specified maximum (0.06 in [1.5 mm]).
- the simulation ran for a specified time (24-hour simulation period for validation tests, one-hour simulation period for final data base).

This procedure was repeated for each combination of outdoor temperature and HRV effectiveness. The outputs from these simulations included energy recovered, ice and frost mass and temperatures, and heat recovery efficiency for each time-step at each simulation temperature.

Running the HRV model for 2°C temperature steps from 10°C (50°F) down to −58°C (−72°F) to a maximum of 60 one-minute time-steps took approximately two hours and forty-five minutes on a PC equipped with a math coprocessor operating at 12 mHz.

TEMPERATURE BIN DATA GENERATOR

The Erbs, Klein, Beckman (EKB) model (Erbs et al. 1983) was used to estimate the number of hours in each temperature bin for one location in each climate studied. The model requires only monthly average temperatures and standard deviations. Bin data generated by the EKB model are sufficiently representative of actual data for this study.

Annual bin data were developed by generating bin data for each month and then summing the number of hours in each temperature bin. Actual bin data for two locations are compared with generated bin data in Figure 4. As shown in the figure, the actual bin data show a significant increase in number of hours for bins near the freezing point of water. The EKB model does not reproduce this phenomenon and also tends to overestimate the number of hours in bins near 60°F (15°C). However, bin hours at low temperatures are relatively well represented, and this was the region of interest for this study.

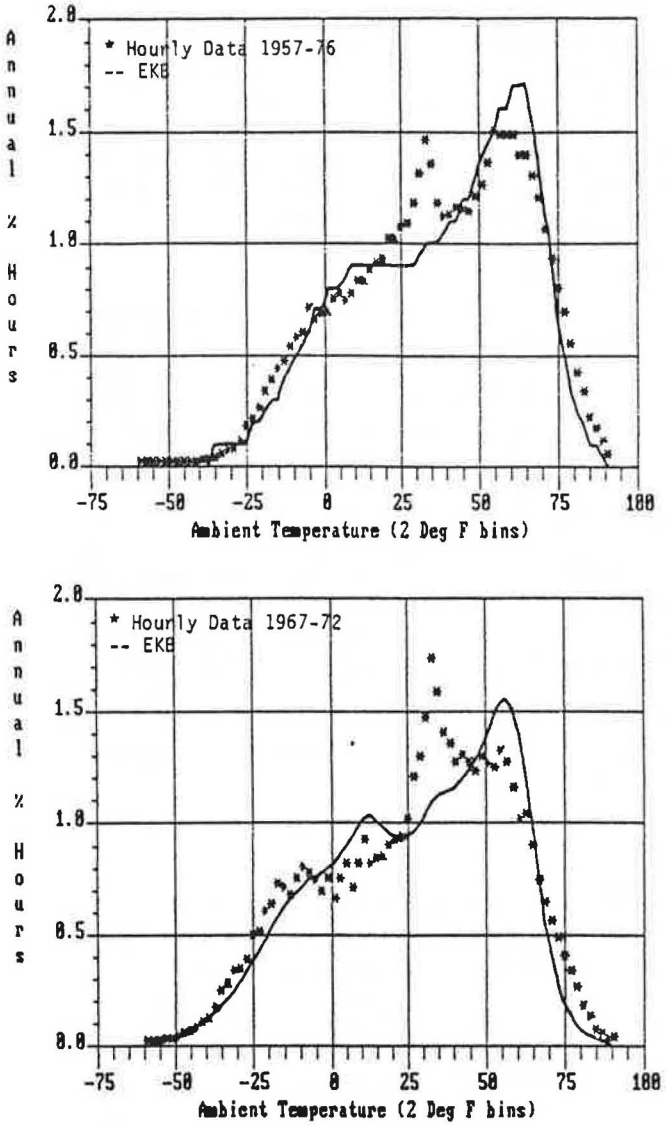

Figure 4 *Actual vs. EKB temperature distribution for Winnipeg, Manitoba (10,600 DDF), and Thompson, Manitoba (14,300 DDF)*

A lower limit for the temperature bin data was selected between the 2½% design temperature and the record low temperature for a given location.

FROST CONTROL AND DEFROST STRATEGY ALGORITHMS

The following describes some common frost control and defrost strategies and the algorithms developed to model them.

Ideal Defrost/Frost Control Strategy

The ideal defrost or frost control strategy would continuously remove frost from heat transfer surfaces without putting energy into the removal process. Thus, heat exchanger fouling would not occur and the latent and sensible energy from cooling and freezing water vapor

would be recovered. This represents the maximum amount of energy that could be recovered in a heat exchanger of a specified effectiveness. This is the standard against which other strategies were compared to determine the upper limit of savings obtainable.

The energy recovery rate from the first time step in a temperature bin (i.e., when heat exchange surfaces are frostfree) was used to calculate the annual energy recovered for the ideal defrost strategy.

Defrost by Supply Fan Shutoff

With this defrost strategy, the outdoor air supply is stopped while exhaust airflow continues uninterrupted. There is no heat recovery from the exhaust air during defrost. The defrost cycle is initiated when outdoor temperatures fall below a preset temperature. The HRV operates in the defrost mode for a set time period (e.g., 5 minutes) at a fixed interval (e.g., every 40 minutes) as long as the outdoor temperature is below the setpoint.

Under mild freezing conditions, the required defrost cycle duration might be one minute per hour, while under severe frosting conditions 10 minutes per hour may be required to melt all ice and frost. Optimization might be achieved by decreasing the length of the defrost cycle or by decreasing the frequency of defrost as supply air temperatures rise.

For this defrost strategy, the heat recovery rate for a temperature bin was calculated as:

$$HRR(T) = AHR(T,t) \times tn/(tn + td) \qquad (13)$$

where

- $HRR(T)$ = heat recovery rate for the defrost strategy defined, in temperature bin T
- $AHR(T,t)$ = average heat recovery rate at time-step t for the heat exchanger operating in temperature bin T (from the HRV simulation data)
- tn = time from the end of one defrost cycle to the beginning of the next defrost cycle (user-specified) (i.e., normal run time)
- td = time from the beginning to the end of a defrost cycle (user-specified) (i.e., time in defrost)

Defrost by Warm Air Recirculation

For this strategy, ventilation is temporarily stopped while house air is recirculated through the HRV to melt ice and frost deposits. Defrost runs for a fixed time (e.g., 2 minutes) at set time intervals (e.g., every 20 minutes) whenever outdoor air temperatures are below the defrost setpoint. To maintain the desired average ventilation rate during cold weather, airflow rates through the heat exchanger must be increased to make up for ventilation lost during the defrost cycle. This increase in airflow will decrease heat exchanger effectiveness.

There is a second energy cost associated with this strategy. The energy needed to melt ice and frost from the heat exchange core is taken from the house air. This "melt" energy must be deducted from the energy already recovered.

For this defrost strategy, the heat recovery rate for a temperature bin was calculated as:

$$HRR(T) = FM \times \{AHR(T,t) - melt\} \qquad (14)$$

where

- $HRR(T)$ = heat recovery rate for the defrost strategy defined, in temperature bin T
- FM = an adjustment factor to reduce the energy recovery rate for increased airflows (user-specified) (values ranged from 0.97 in the Arctic to 1.0 in the Pacific climate zone)
- $AHR(T,t)$ = average heat recovery rate at time-step t for the heat exchanger operating in temperature bin T (from the HRV simulation data)
- $melt$ = the energy required to melt the frost and ice accumulated at the end of time-step t (from the HRV simulation data)

Frost Control by Supply Air Preheat

Frosting conditions in the heat exchange core can be avoided by heating supply air above the frost threshold temperature before it enters the heat exchange core. Continuous ventilation can be maintained without airflow imbalances. Block-switched and variable-output heater controls were modeled.

With block-switched controls, heater output is changed in blocks (e.g., 1 kW). This results in a known supply air temperature increase ($Tinc$) when a block heater is switched on. The energy recovery rate used for temperature bin T is the energy recovery rate for temperature bin $T + Tinc$. Preheat energy was calculated by multiplying the heater capacity (in kW) by the number of hours in the temperature bin.

The optimum preheater varies its output, maintaining the supply air temperature just above the frost threshold temperature. The heat recovery rate for the temperature just above the frost threshold was utilized in all temperature bins below the frost threshold temperature (i.e., it was assumed that the supply air was heated to the frost threshold temperature for all temperature bins below the frost threshold). Preheat energy was calculated as the increase in enthalpy needed to raise air from the bin temperature to the frost threshold temperature, multiplied by the mass flow rate of the supply airstream.

Frost Control by Reducing Heat Exchange Effectiveness

Tilting heat pipes and reducing heat wheel speeds reduces their effectiveness and can be used to prevent frosting. The objective is to prevent condensation onto cold heat exchanger surfaces. Whenever core or wheel temperatures are below freezing, the exhaust airstream exit temperature must be kept above its dew point. At these times, the energy recovery rate is the difference between the enthalpy of the exhaust air at its inlet conditions and its dew point multiplied by the exhaust air mass flow rate.

Frost Control by Reducing Supply Airflow Rates

Reducing the supply airflow relative to the exhaust airflow is another method of preventing frost or ice from

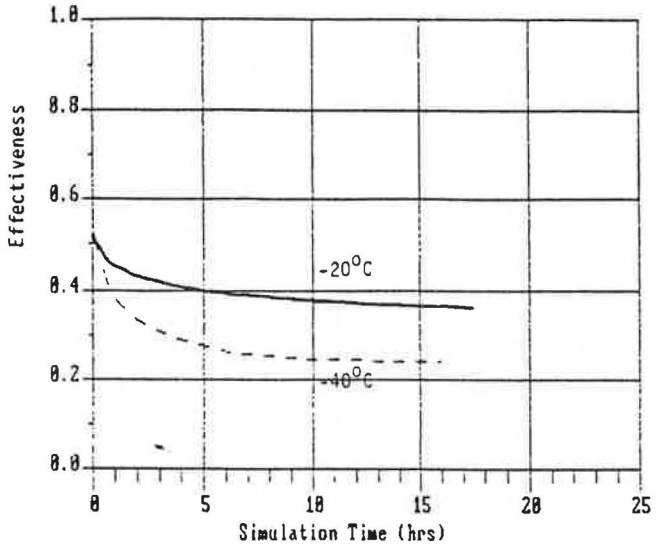

Figure 5 *Predicted effectiveness vs. operating time (without defrost) for a nominal 50% effective HRV operating with indoor air at 68°F (20°C) and 40% RH and outdoor air at −4°F (−20°C) and −40°F (−40°C)*

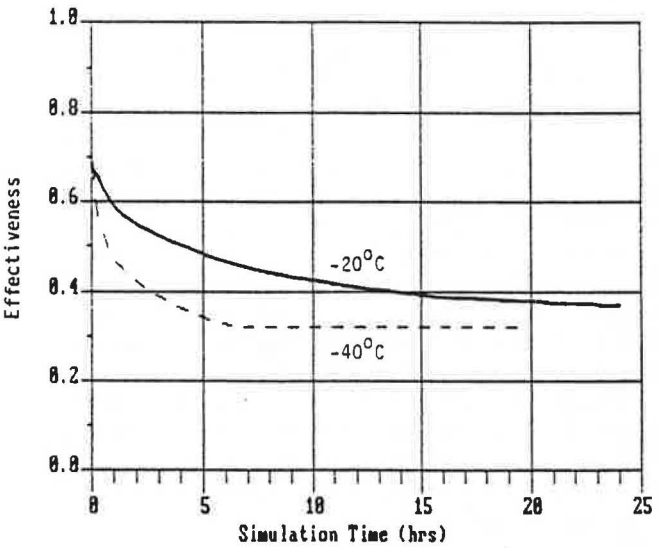

Figure 6 *Predicted effectiveness vs. operating time (without defrost) for a nominal 65% effective HRV operating with indoor air at 68°F (20°C) and 40% RH and outdoor air at −4°F (−20°C) and −40°F (−40°C)*

forming in the heat exchange core. The energy recovery rate using this strategy during frosting conditions was estimated as:

$$ETRANS = m \times (H1 - HDP) \quad (15)$$

where

ETRANS = energy that can be transferred from the exhaust airstream
m = exhaust air mass flow rate
H1 = inlet exhaust air enthalpy
HDP = enthalpy at the dew point of the exhaust airstream

The supply airflow rate for a given bin temperature was estimated as follows:

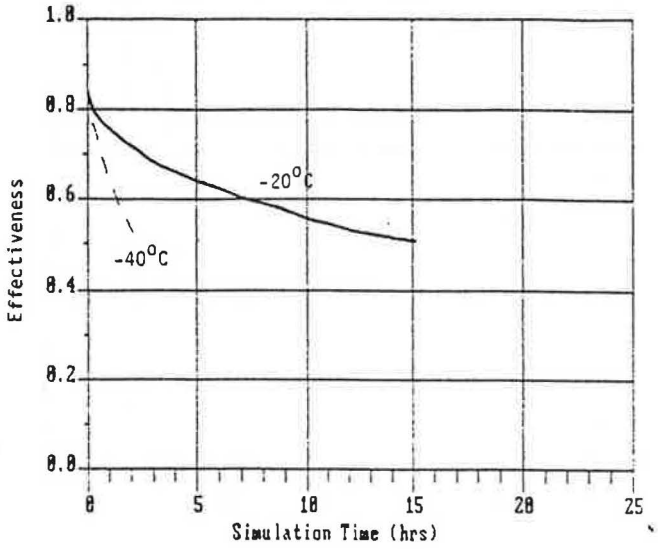

Figure 7 *Predicted effectiveness vs. operating time (without defrost) for a nominal 80% effective HRV operating with indoor air at 68°F (20°C) and 40% RH and outdoor air at −4°F (−20°C) and −40°F (−40°C)*

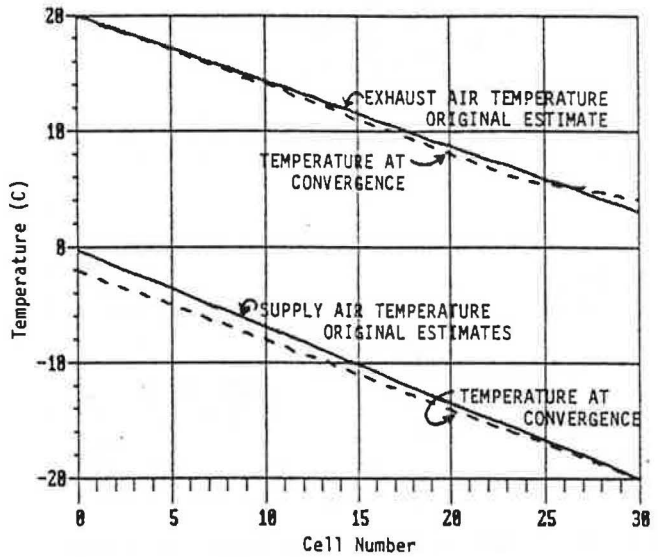

Figure 8 *Predicted cell temperature profiles for a nominal 50% effective HRV operating with indoor air at 68°F (20°C) and 40% RH and an outdoor temperature of −4°F (−20°C)*

1. The temperature and enthalpy rise of the supply airstream passing through the heat exchanger was estimated using the nominal heat exchanger effectiveness.
2. The allowable mass flow rate of exhaust air was estimated by dividing the allowable energy transfer, *ETRANS*, by the change in enthalpy of the exhaust airstream.

POST PROCESSOR

The "post processor" merged the weather data and time-step/temperature data from the HRV frosting model simulations with the defrost and frost control algorithms to predict the energy recovered by heat exchangers of various effectivenesses, operating in various climatic con-

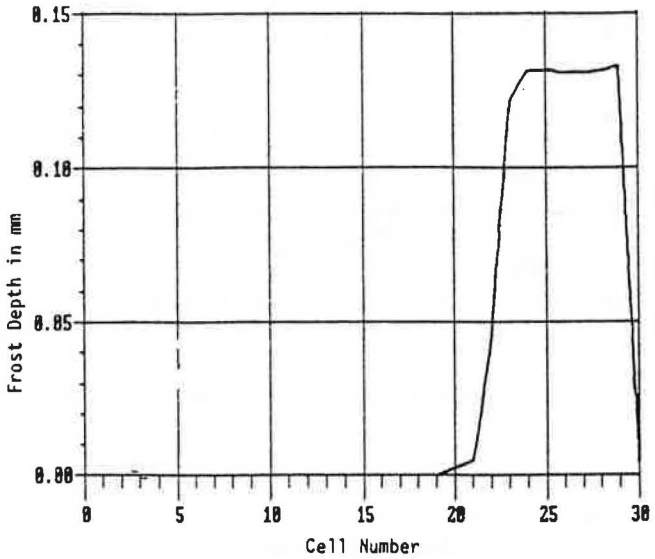

Figure 9 *Predicted frost depth profiles for a nominal 50% effective HRV after one hour of operation with indoor air at 68°F (20°C) and 40% RH and an outdoor temperature of −4°F (−20°C)*

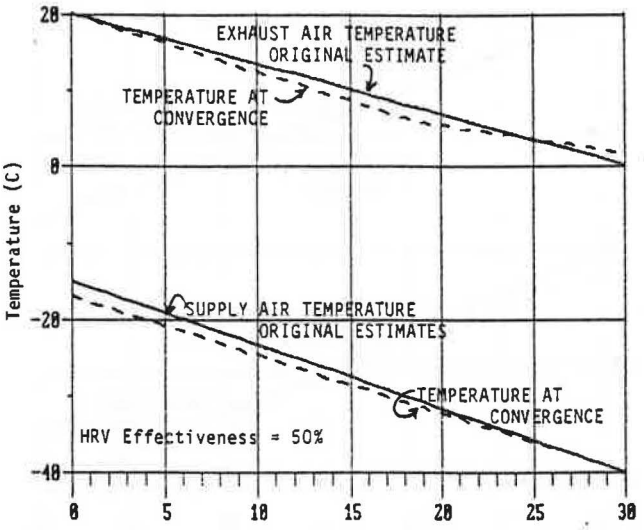

Figure 10 *Predicted cell temperature profiles for a nominal 50% effective HRV operating with indoor air at 68°F (2°C) and 40% RH and an outdoor temperature of −40°F (−40°C)*

ditions, and using various defrost and frost control strategies.

Whereas the computer time needed to perform a heat exchanger simulation was long (typically two hours), the computer time needed to evaluate a defrost or frost control strategy for a given climatic condition was less than five seconds. All the variations simulated can be compared on the standardized basis of annual energy recovered (i.e., energy savings).

RESULTS AND CONCLUSIONS

Performance data of various simulation results were printed and plotted to assist in debugging the program. Selected data plots are presented in Figures 5 through 11.

Figures 5, 6, and 7 show simulated HRV effectiveness over time at selected simulation temperatures. The simu-

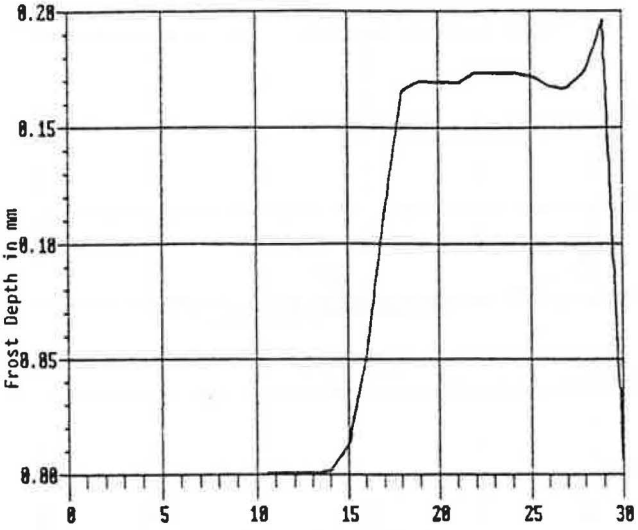

Figure 11 *Predicted frost depth profiles for a nominal 50% effective HRV after one hour of operation with indoor air at 68°F (20°C) and 40% RH and an outdoor temperature of −40°F (−40°C)*

lations continued until one of the following conditions was met:

1. Simulation time exceeded 24 hours.
2. The maximum thickness of frost or ice in any cell exceeded 0.06 in (1.5 mm) (plugged).
3. Steady-state was reached.

In the −4°F (−20°C) simulation, steady-state was reached after approximately 18 hours for the 50% effective HRV. The 65% effective HRV ran the full 24-hour period without reaching steady state. The 80% HRV exceeded the allowable frost thickness after 14 hours. At the −40°F (−40°C) simulation condition, all simulations terminated on the frost thickness criteria. The 50% HRV model stopped after 16 hours, the 65% HRV model after 19 hours, and the 80% model "plugged" after 2.5 hours.

Figures 8 and 10 plot temperature profiles for the first time-step of the 50% effective HRV at −4°F (−20°C) and −40°F (−40°C). Figures 9 and 11 show the frost thickness in each cell after a one-hour simulation period for the same heat exchanger conditions.

The results of the HRV frosting simulations appeared reasonable for the intended use. The intended use of these results was to provide a data base from which comparisons of the relative performance of freeze control strategies could be made (not to develop, test, and prove an HRV frosting model). The limited availability of empirical data prevents one from drawing conclusions regarding the accuracy of the model. However, it is believed that this does not detract from the validity of the comparisons made of HRV freeze control strategies in the study.

The literature search revealed a multiplicity of mathematical expressions for effectiveness, sensible effectiveness, and heat recovery efficiency, indicating a need for standardization of nomenclature relating to air-to-air energy recovery.

REFERENCES

Alexander, R.C. 1986. "Comparison of performance indices for heat recovery ventilators." *ASHRAE Transactions*, Vol. 92, Part 2A.

Barringer, C.G., and McGugan, C.A. 1988. "Investigation of enthalpy air-to-air residential heat exchangers." Final report for ASHRAE Research Project 544-RP, September 26.

Besant, R.W., and Bugg, J.D. 1982. "The performance of a counterflow air-to-air heat exchanger with water vapour condensing and frosting." Department of Mechanical Engineering, University of Saskatchewan.

Biguria, G., and Wenzel, L. 1970. "Measurement and correlation of water frost thermal conductivity and density." *Industrial and Engineering Chemistry Fundamentals*, Vol. 9, No. 1, p. 129.

Erbs, D.G.; Klein, S.A.; and Beckman, W.A. 1983. "Estimation of degree day on ambient temperature bin data from monthly average temperatures." *ASHRAE Journal*, June, pp. 60-65.

Fisk, W.J.; Archer, K.M.; Chant, R.E.; Offermann, F.J.; Hekmant, D.; and Pedersen, B.S. 1983. "Freezing in residential air-to-air heat exchangers: an experimental study." Lawerence Berkeley Laboratory, Report LBL-16783, September.

Fisk, W.J.; Archer, K.M.; Offermann, F.J.; Chant, R.E.; Hekmat, D.; and Pedersen, B.S. 1985a. "Performance of residential air-to-air heat exchangers during operation with freezing and periodic defrosts." *ASHRAE Transactions*, Vol. 91, Part 1B.

Fisk, W.J.; Chant, R.E.; Archer, K.M.; Offermann, F.J.; Hekmat, D.; and Pedersen, B.S. 1985b. "Onset of freezing in residential air-to-air heat exchangers." *ASHRAE Transactions*, Vol. 91, Part 1B.

Hayashi, Y.; Aoki, K.; and Yuhara, H. 1977. "Study of frost formation based on theoretical model of the frost layer." *Heat Transfer Japanese Research*, Vol. 6.

Jones, B.W., and Parker, J.D. 1975. "Frost formation with varying environmental parameters." *Transactions of the ASME Journal of Heat Transfer*, Vol. 97, p. 255.

Kamei, S.; Mitzushina, T.; Kilune, S.; and Koto, T. 1952. "Research on the frost formation in low temperature cooler condenser." *Japan Sci. Rev.*, Vol. 2.

Nisson, N. 1984. "Air-to-air heat exchanger: testing for effectiveness." *Energy Design Update*, Vol. 3.

Ontario Ministry of Energy. 1987. "Monitoring of R-2000 low energy homes." *Annual Report.*

Phillips, E.G.; Fisher, D.R.; Chant, R.E.; and Bradley, B.C. 1989. "Comparison of freezing control strategies for residential air-to-air, heat recovery ventilators." *ASHRAE Transactions*, Vol. 95, Part 2 (in press).

Schneider, H.W. 1978. "The equation of the growth rate of frost forming on cooled surfaces." *Transactions of the ASME Journal of Heat and Mass Transfer*, Vol. 21, p. 1019.

Yonko, J.D., and Sepsy, C.F. 1967. "An investigation of the thermal conductivity of frost while forming on a flat horizontal plate." *ASHRAE Transactions*, Vol. 73, Part 2.